Separation Science and Technology
Publication details, including instructions for authors and subscription information:
http://www.informaworld.com/smpp/title~content=t713708471

Comparison of Breakthrough Performance Using Dye-Affinity Membrane Disks and Gel Bead Columns

Shing -Yi Suen[a]; Yueh -Hua Tsai[a]; Rui -Long Chen[a]
[a] DEPARTMENT OF CHEMICAL ENGINEERING, NATIONAL CHUNG HSING UNIVERSITY, TAICHUNG, TAIWAN, REPUBLIC OF CHINA

Online publication date: 20 March 2000

To cite this Article Suen, Shing -Yi , Tsai, Yueh -Hua and Chen, Rui -Long(2000) 'Comparison of Breakthrough Performance Using Dye-Affinity Membrane Disks and Gel Bead Columns', Separation Science and Technology, 35: 4, 573 — 591
To link to this Article: DOI: 10.1081/SS-100100177
URL: http://dx.doi.org/10.1081/SS-100100177

SEPARATION SCIENCE AND TECHNOLOGY, **35**(4), pp. 573–591, 2000

Comparison of Breakthrough Performance Using Dye-Affinity Membrane Disks and Gel Bead Columns

SHING-YI SUEN,* YUEH-HUA TSAI, and RUI-LONG CHEN
DEPARTMENT OF CHEMICAL ENGINEERING
NATIONAL CHUNG HSING UNIVERSITY
TAICHUNG, TAIWAN 402, REPUBLIC OF CHINA

ABSTRACT

The breakthrough curve performance of lysozyme and bovine serum albumin to immobilized Cibacron Blue 3GA using different solid supports such as gel beads and membrane disks was investigated in this work. The effects of flow rate and different module designs were also studied. Variation in the flow rate was found to be insignificant for the column process in both nonadsorption and single-protein experiments, but it affected the elution peak height for membrane disks. The peak height decreased with increasing flow rate. As for the effect of different designs, a long column and a wide membrane stack induced a broader breakthrough performance. The performance varied with different solid supports in two-protein experiments. Competitive adsorption occurred for a gel bead column, and the breakthrough curve performance resembled the prediction of combining local equilibrium theory and the extra module effect. The affinity strength to the gel bead support is in the order lysozyme $>$ BSA dimer $>$ BSA monomer. As for membrane performance, two BSA solutes did not adsorb onto membranes, so a simple separation of lysozyme from BSA, instead of displacement phenomena, was observed.

INTRODUCTION

Due to its high specificity, affinity adsorption and chromatography has become a popular separation technique for biomolecule purification applications. Conventional affinity chromatography is carried out in columns packed

* To whom correspondence should be addressed. FAX: 886-4-2854734. E-mail: sysuen@nchu.edu.tw

with porous beads onto which the ligand is immobilized. However, separation performance in packed columns is usually limited by either slow intraparticle diffusion or high column pressure drops and low flow rates. Recently, the use of a membrane as the solid support has demonstrated its potential in overcoming these severe mass-transfer limitations (1–6). Low transmembrane pressure drops and high flow rates reduce the required time for a separation cycle and, as a result, raise the economic efficiency. Therefore, the advantages in mass transfer and economic cost propel the choice of a membrane as the solid support to replace the traditional column.

Different types of membrane have been employed for the adsorption process, and a membrane disk is the most frequently utilized and well studied in the literature. The major advantages of using membrane disk come from the fact that its commercial products are of various sizes and materials, which can provide more choices for users to meet their needs. Moreover, the design of a disk holder is simpler and the cost for both the holder and membrane itself is lower compared to other types of membrane. Accordingly, many studies have attempted to improve and extend the applications of adsorptive membrane disks (2–4, 7–14). However, in most research the membrane performance has not been compared to traditional column techniques. Without practical comparison of the adsorption properties and separation performance for the same biomolecule system using adsorptive membranes and conventional beads, it is difficult to provide extensive information for selecting the best solid support in different practical cases.

It is worthy to recall that the main driving force for affinity separation is either the affinity strength or the intrinsic adsorption rate constant of biomolecule onto the ligand on the solid support. These affinity adsorption properties usually dominate the final separation performance and the design of operating flow conditions and, accordingly, become the key factors for affinity chromatography techniques. Conventionally, the adsorption behavior for the same ligand–biomolecule system is considered similar, even if different solid supports such as membranes and porous beads are used. However, distinct adsorption properties have been observed for the same system through the use of different solid supports (gel beads and membrane disks) in previous work by the author (15). These different adsorption properties may subsequently lead to different breakthrough performances, which requires further extensive studies. Therefore, the objective of this work was to measure and compare the breakthrough curves of two proteins (lysozyme and bovine serum albumin) to an immobilized ligand (Cibacron Blue 3GA) using both gel beads and membrane disks together with suitable modules. Different designs and operating conditions were tested to decide the optimal conditions for a better choice of solid support.

EXPERIMENTAL

Materials

Two kinds of solid support, gel beads and membrane disks, are studied in this work. Blue Sepharose CL-6B from Pharmacia Biotech AB (Uppsala, Sweden), on which the ligand Cibacron Blue 3GA is immobilized, was used as gel beads. Blue Sepharose CL-6B was packed in two columns of different size (G10×250 and G16×150) from Amicon Company (Beverly, MA, USA) for breakthrough curve measurements. The membrane disks used are regenerated cellulose filters of 80 μm thickness and 0.45 μm pore size from Sartorius AG (Goettingen, Germany). Two disk holders were used for 25 and 47 mm disks, respectively, in the breakthrough curve experiments. The basic properties for the solid supports and modules are shown in Table 1.

TABLE 1
Basic Properties of Solid Supports and Modules Used in This Work

Solid supports		
	Gel beads	Membrane disks
Material	Crosslinked agarose	Regenerated cellulose
Density	1.58 g/cm^3[a]	—
Diameter	45–165 μm (wet) (bead swelling in distilled water: 4–5 cm^3/g)	25 and 47 mm
Specific surface area	0.45 m^2/g[a]	—
Porosity	0.00094 (dry)[a]	0.45 (min. 0.36 ~ max. 0.67)
Temperature stability	4–40°C	Up to 180°C
pH stability	4–12	—
Modules		
	Gel bead columns	Membrane disk holders
Material	Glass	Acrylic
Diameter	Column 1: 10 mm Column 2: 16 mm	Holder 1: 25 mm Holder 2: 47 mm
Adjustable height	Column 1: up to 250 mm Column 2: up to 150 mm	Holder 1: up to 50 disks Holder 2: up to 50 disks
Pressure rating	Column 1: 7 bar Column 2: 6 bar	—

[a] Data obtained by surface area and pore size analyzer (BET method).

MARCEL DEKKER, INC.
270 Madison Avenue, New York, New York 10016

Cibacron Blue 3GA (C9534), chicken egg white lysozyme (L6876, MW = 14,300) and BSA (A3059, MW = 67,000) were purchased from Sigma Chemical (St. Louis, MO, USA). The loading buffer for protein adsorption was 50 mM Tris-HCl, pH 7, with 0.005% NaN_3. The elution buffer was 1 M KCl in Tris-HCl. Both buffers were filtered through 0.2 μm nylon membranes (Lida Manufacturing, Kenosha, WI, USA). Protein solutions were filtered by 0.45 μm filters (F9888, Sigma Chemical).

Ligand Immobilization onto Membrane Disks

The method presented by Liu and Fried (9) was utilized for the coupling of triazine dye Cibacron Blue 3GA with the active OH groups of the regenerated cellulose membranes.

Batch Adsorption Experiments

Batch adsorption experiments were conducted at room temperature. The detailed procedures can be found in a previous paper by the author (15).

Breakthrough Curve Experiments

The equipment for breakthrough curve experiments included a peristaltic pump (AC-2120 PERISTA BIO-MINIPUMP, ATTO, Tokyo, Japan), a UV detector with a built-in chart recorder (UA-6, ISCO, Lincoln, NE, USA), and a datalogger (ESCORT, Cox Technologies, Belmont, NC, USA). The protein absorbance was detected at 280 nm. A fraction collector (Retriever 500, ISCO) was used to collect effluent samples for the two-protein separations. All experiments were conducted at room temperature.

For column experiments, gel beads were packed inside the column to a desired height. For membrane disk experiments, membrane disks were placed in the suitable holder and the holder was screwed very tightly. An O-ring was used to prevent fluid from lateral leaking. Prior to each experiment the gel bead column or membrane cartridge was cleaned and regenerated with loading buffer. All the experimental settings and operating conditions are listed in Table 2. Each experiment, except for the two-protein ones, was repeated twice.

Nonadsorption Experiments

Nonadsorption experiments were conducted using 0.18 mg/mL lysozyme in pure elution buffer. The gel bead column or membrane disk holder was first equilibrated with elution buffer, then the protein solution was loaded, and the absorbance was recorded by the datalogger. Until the raised absorbance was steady, elution buffer was loaded as washing buffer to bring the absorbance curve back to baseline.

TABLE 2
Experimental Conditions for Column and Membrane Operations

Basic Settings

	Column			Membrane		
	A	B	C	D	E	F
Diameter (mm)	16	10	10	47	25	25
Height	6.5 cm	6.5 cm	16.6 cm	11 disks	11 disks	40 disks
Bed volume (cm^3)	13	5.1	13	1.53	0.43	1.57
Bed porosity	—	—	0.9	0.45[a]	0.45[a]	0.45[a]
Flow rate (mL/min)	0.5, 1	0.5, 1	0.5, 1	0.5, 1, 5	0.5, 1, 5	0.5, 1, 5

Beginning Time of Each Stage (as effluent volume, mL)

For all the experiments, the loading stage started at 0 mL

(*a*) *Nonadsorption Experiments*

Stage	Flow rate (mL/min)	Column A	Column B	Column C	Membrane D	Membrane E	Membrane F
Washing (elution buffer)	0.5	76.5	54	82	75	55	54
	1	82	53	82	75	55	54
	5	—	—	—	75	55	54

(*b*) *Single-Protein Experiments*

Stage	Flow rate (mL/min)	Column A	Column B	Column C	Membrane D	Membrane E	Membrane F
Washing (loading buffer)	0.5	86.5	52.5	84	65	40	60
	1	93	55	93	65	40	60
	5	—	—	—	65	40	60
Elution (elution buffer)	0.5	131	100.5	445.5	160	100	140
	1	154	130	318	160	100	140
	5	—	—	—	160	100	140

(*c*) *Two-Protein Experiments*

Stage	Flow rate (mL/min)	Column B	Membrane E
Washing (loading buffer)	1	100	40
Elution (elution buffer)	1	300	103

[a] See Table 1.

MARCEL DEKKER, INC.
270 Madison Avenue, New York, New York 10016

Single-Protein Experiments

The gel bead column or membrane disk holder was first equilibrated with loading buffer, followed by loading the protein solution. A high feed concentration was necessary to saturate the column system. Consequently, a concentration of 3.75 mg/mL lysozyme in loading buffer was adopted in this experiment. The protein absorbance was detected and then recorded by the datalogger. After the absorbance no longer increased, loading buffer was pumped through as washing buffer until the absorbance returned to baseline. Elution buffer was then used to elute the bound protein from the system, and this elution process was finally stopped when the absorbance returned to baseline.

Two-Protein Experiments

In the two-protein experiments, feed concentrations of 2 mg/mL lysozyme and 2 mg/mL BSA and a flow rate of 1 mL/min were used. The operating stages are similar to those for single-protein experiments, and the settings are listed in Table 2. The fractions of effluent solution were collected by the fraction collector and analyzed under 280 nm using the FPLC system (Pharmacia Biotech AB) composed of a controller (LCC-501), a pump (P-500), a UV detector (UV-1), and a gel filtration column (Superose 6HR 10/30). The mobile phase used was 0.1 M Tris-HCl, pH 7.4, with 0.005% NaN_3. The sample amount for each injection was 100 μL. The mobile phase flow rate was 0.42 mL/min.

RESULTS AND DISCUSSION

Batch Adsorption Performance

Batch adsorption experiments at room temperature were conducted and reported in an earlier paper by the author (15). It was found that BSA did not adsorb onto Cibacron Blue 3GA-immobilized membrane disks, which may be due to the effects of blocking or steric hindrance as reported in the literature (14, 15). The Langmuir model was used to fit the experimental isotherm data:

$$c_s = \frac{cc_l}{K_d + c}$$

The fitted parameter values for gel beads were: $c_l = 2100 \pm 200$ μM and $K_d = 6.8 \pm 1.8$ μM for lysozyme; $c_l = 210 \pm 10$ μM and $K_d = 4 \pm 1$ μM for BSA. The adsorption property values of lysozyme for membrane disks were: $c_l = 1400 \pm 70$ μM and $K_d = 1.4 \pm 0.4$ μM. Comparing these values, lysozyme displayed a slightly lower saturation capacity but a higher affinity strength (reciprocal of dissociation equilibrium constant) for mem-

brane disks as the solid support. Moreover, BSA had a much lower capacity (1/10) but a higher affinity strength than lysozyme in the case of gel beads as the solid support.

Nonadsorption Breakthrough Curves

In the nonadsorption experiments, 0.18 mg/mL lysozyme (12.6 μM) in elution buffer was loaded and then emerged into the effluent without adsorption. Three designs with different size and height were used for both the gel bead column and membrane disk holder: wide and short, narrow and short, narrow and long. Table 2 summarizes all the setting data and solution volumes used. The highest available flow rates were 1 and 5 mL/min for the gel bead columns and membrane holders, respectively, due to the limitation of experimental equipment and module height.

The breakthrough curve performance for nonadsorption experiments is presented in Fig. 1. It can be observed from the results that the variation in flow rate did not influence the breakthrough curves. Moreover, by comparing panels 1A–1C with panels 1D–1F, the nonadsorption breakthrough curves of the gel bead columns were broader than those of the membrane holders in both loading and washing stages. To explain these phenomena, the possible mass-transfer effects in both column and membrane processes need to be investigated. The mass-transfer effects contributing to a nonadsorption breakthrough curve can be divided into two parts: inside-module effects and extra-module effects. The extra-module effects include the delay volume effect from the fluid flowing through the tubing and the detector flow cell and the dead-volume mixing effect (3, 10). In this work the extra-module design, such as tubing material, tubing diameter, tubing length, and the detector, was not altered in the experiments. Therefore, the extra-module effects should be identical for all cases, and the difference between the column and membrane processes should come from different inside-module mass-transfer effects for the different modules used.

Axial diffusion, boundary-layer mass transfer (BLMT), and intraparticle diffusion are the important mass-transfer effects occurring inside the chromatographic column, but intraparticle diffusion does not exist in the membrane system. To investigate the significance of these effects, the time scales for these effects were calculated and compared to the convection time scale (L/v). For the axial diffusion effect, the calculated values of the axial Peclet number (vL/D), determined by using the data of molecular diffusion coefficient of lysozyme in the literature (16), were found to be far above 40 in all cases. This means that the time scale for axial diffusion (L^2/D) was much longer than the convection time (17). Therefore, the axial diffusion effect was not significant. The BLMT time scale has various definitions for different solid supports. Assuming that the solute has to pass through a mass-

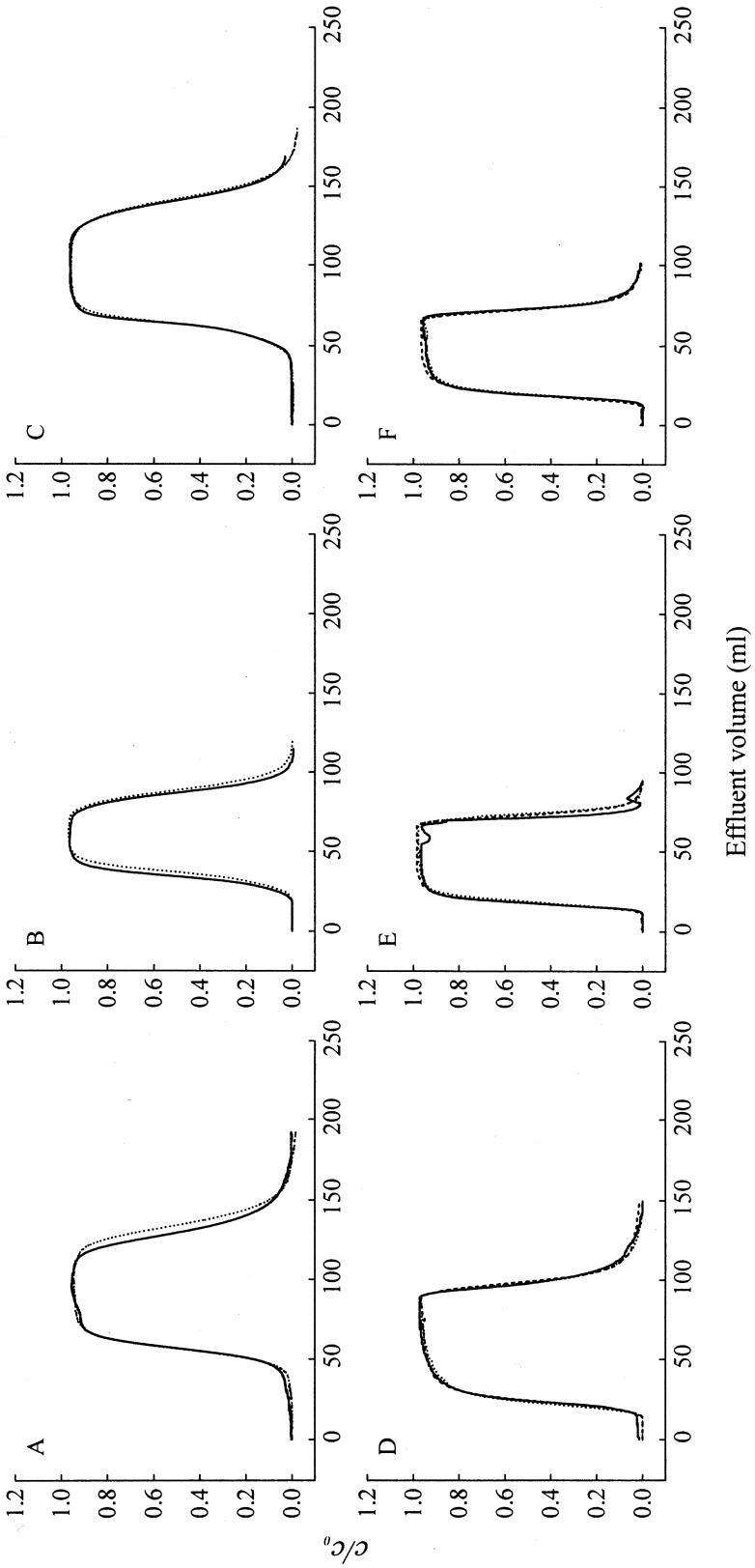

FIG. 1 Effect of flow rate on the breakthrough curves for nonadsorption experiments. Solid line = 0.5 mL/min; dotted line = 1 mL/min; dashed line = 5 mL/min. The settings for A to F are described in Table 2.

MARCEL DEKKER, INC.
270 Madison Avenue, New York, New York 10016

transfer film surrounding the outer surface of the particle to reach the particle support, it may be defined as D_p/k_c for a particle-packed bed. As for the membrane structure, the BLMT time scale may be estimated as D_p/k_c because the solute would pass the mass-transfer film in the radial direction inside the membrane pore and then reach the pore wall. Using a simple correlation for BLMT coefficient k_c, $D_p k_c/D = 4$ for column and $d_p k_c/D = 4$ for membrane (17), the estimated time scale was 0.1–1.7 minutes for the column process and 1×10^{-5} minutes for the membrane process. The time scale of intraparticle diffusion for the column process, defined as $D_p^2/4D$, was the same as the BLMT time scale used here. The convection time scale for the column process (4–23 minutes) was around 10 times its corresponding time scale of BLMT and intraparticle diffusion, whereas the convection time scale for the membrane process (0.04–1.4 minutes) was much greater than its BLMT time scale. Accordingly, the effect of BLMT was negligible in the membrane process, but both the effects of BLMT and intraparticle diffusion in the column process could not be neglected and should have resulted in a broader breakthrough curve.

To evaluate the effects using different sizes and heights of columns and holders, the nonadsorption results for the same flow rate but different settings were replotted in Fig. 2. From the results in panels 2(a) and 2(b), the protein emerged earliest and also washed out earliest in the case of the lowest bed volume (setting B: narrow and short column). This is mainly due to the reduction of the system dead volume (including the void volume of the bed) in the case of the lower column volume. However, for cases with the same bed volume but a different column design such as setting A (wide and short column) and setting C (narrow and long column), the nonadsorption results are different. An extra volume was needed for the solute to emerge in the loading stage for setting C. In other words, setting C showed a worse breakthrough performance than setting A. Conclusively, bed length was the dominant factor affecting nonadsorption column performance.

As to the membrane performance, the results are shown in panels 2(c) to 2(e). It should be noted that the membrane holders used in this work can accommodate up to 50 regenerated cellulose disks. However, to minimize the destruction of the frontal membrane by tight screwing, the use of up to 40 disks is more appropriate and has been adopted in setting F. Due to the small thickness of membrane disks, all the bed volume values and hence the bed void volume values were very low. Therefore, the effluent volume for protein to emerge was very close for different settings, as shown in Figs. 2(c) to 2(e). Even so, a wide membrane stack (setting D) still displayed a broader breakthrough curve than narrow membrane stacks (settings E and F). This indicates that membrane disk diameter was the dominant factor in nonadsorption breakthrough curves.

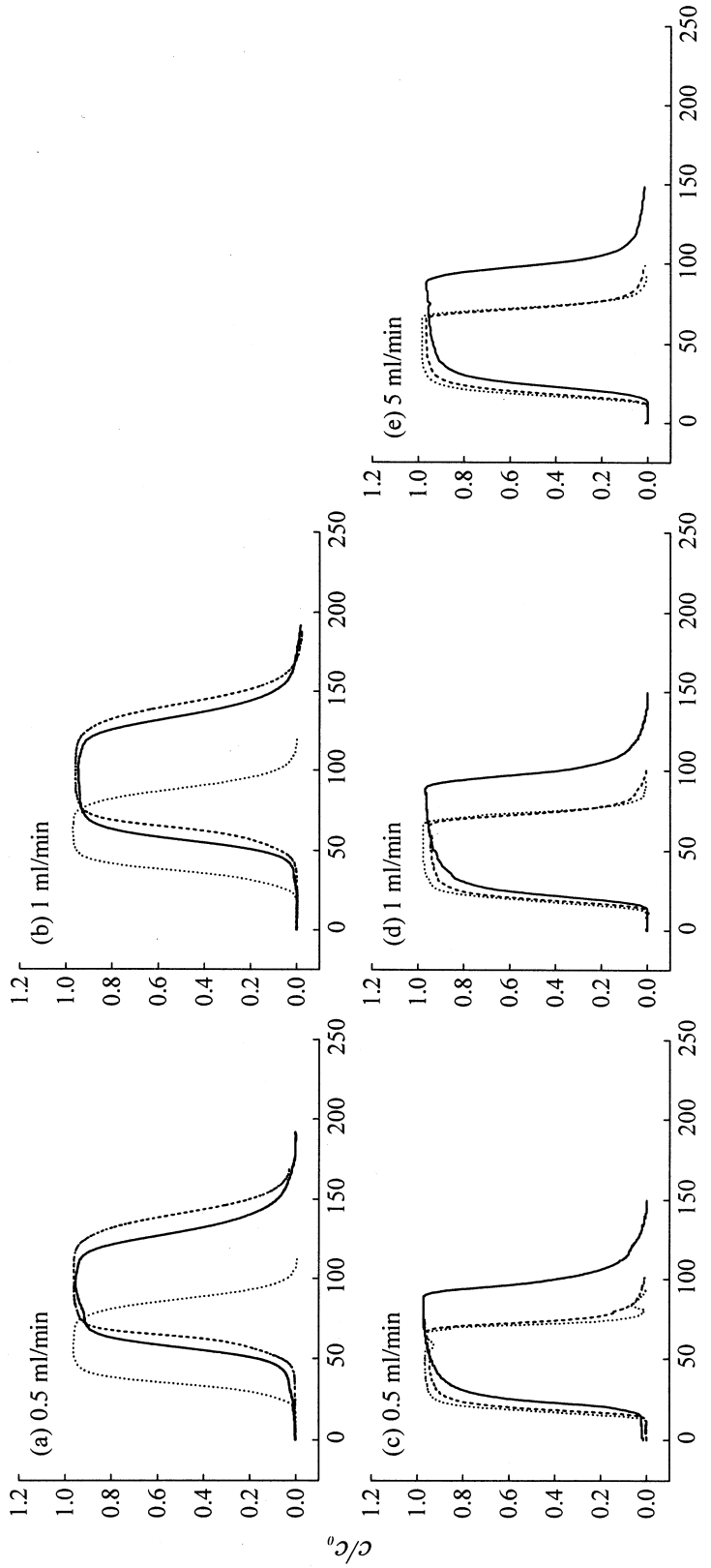

FIG. 2 Effect of different module designs on the breakthrough curves for nonadsorption experiments. For (a) and (b), solid line = setting A (wide and short column); dotted line = setting B (narrow and short column); dashed line = setting C (narrow and long column). For (c) to (e), solid line = setting D (wide and thin membrane stack); dotted line = setting E (narrow and thin membrane stack); dashed line = setting F (narrow and thick membrane stack). The settings for A to F are described in Table 2.

MARCEL DEKKER, INC.
270 Madison Avenue, New York, New York 10016

Single-Protein Breakthrough Curves

Figure 3 contains experimental single-protein breakthrough curves for 3.75 mg/mL lysozyme (262 μM) in loading buffer at various flow rates and designs of column and membranes. Note that different volumes in the loading or washing stage were used at different flow rates for gel bead columns, as shown in Table 2(b), and resulted in differences in the emergence of the washing curve or elution peak. If these differences are filtered out, the effect of flow rate would become insignificant. As to the membrane performance, the effect of flow rate can be observed from the variation in elution peak height, especially in the case of setting E (narrow and short membrane). When the flow rate increased, the peak height decreased. Based on the area under the elution peak, the eluted protein amount was slightly reduced with increasing flow rate. This effect is similar to those reported in the literature (2, 10).

Similar to nonadsorption experiments, the single-protein results were replotted and are illustrated in Fig. 4 to investigate the effects of different designs. In panels 4(a) and 4(b), the protein emerged and eluted out earliest in the case of the lowest bed volume (setting B), similar to the nonadsorption experiments. As for the comparison between settings A and C (same bed volume but different column design), the effluent concentration for setting A (wide and short column) rose earlier in the loading stage and also returned to a stable baseline earlier in the washing stage. The washing stage was particularly lengthened in the case of setting C (narrow and long column). That is, extra broadening volume was necessary for a longer column in both the loading and washing stages. As to the elution peak height, the apparent height differed at various column settings. However, these differences basically resulted from the change of baseline level after the washing stage and can hardly be compared. Conclusively, similar to the nonadsorption results, bed length dominated the single-protein breakthrough performance.

The results for membrane performance were replotted in panels 4(c) to 4(e). The order for protein emergence from earliest to last in the loading stage was setting E, F, and D. Moreover, setting D (wide and short membrane stack) presented the lowest risen concentration and a broader washing curve than settings E and F (narrow membrane stacks). Accordingly, a wide membrane stack resulted in the worst mass-transfer and breakthrough performance.

Two-Protein Breakthrough Curves

Experimental two-protein breakthrough curves for a feed solution containing 2 mg/mL lysozyme (140 μM) and 2 mg/mL BSA (30 μM) at 1 mL/min are presented in Figs. 5 and 6 for a gel bead column and a membrane disk holder, respectively. Only settings B and E were used. The two-protein solution was essentially a ternary-solute solution because approximately 25% of

MARCEL DEKKER, INC.
270 Madison Avenue, New York, New York 10016

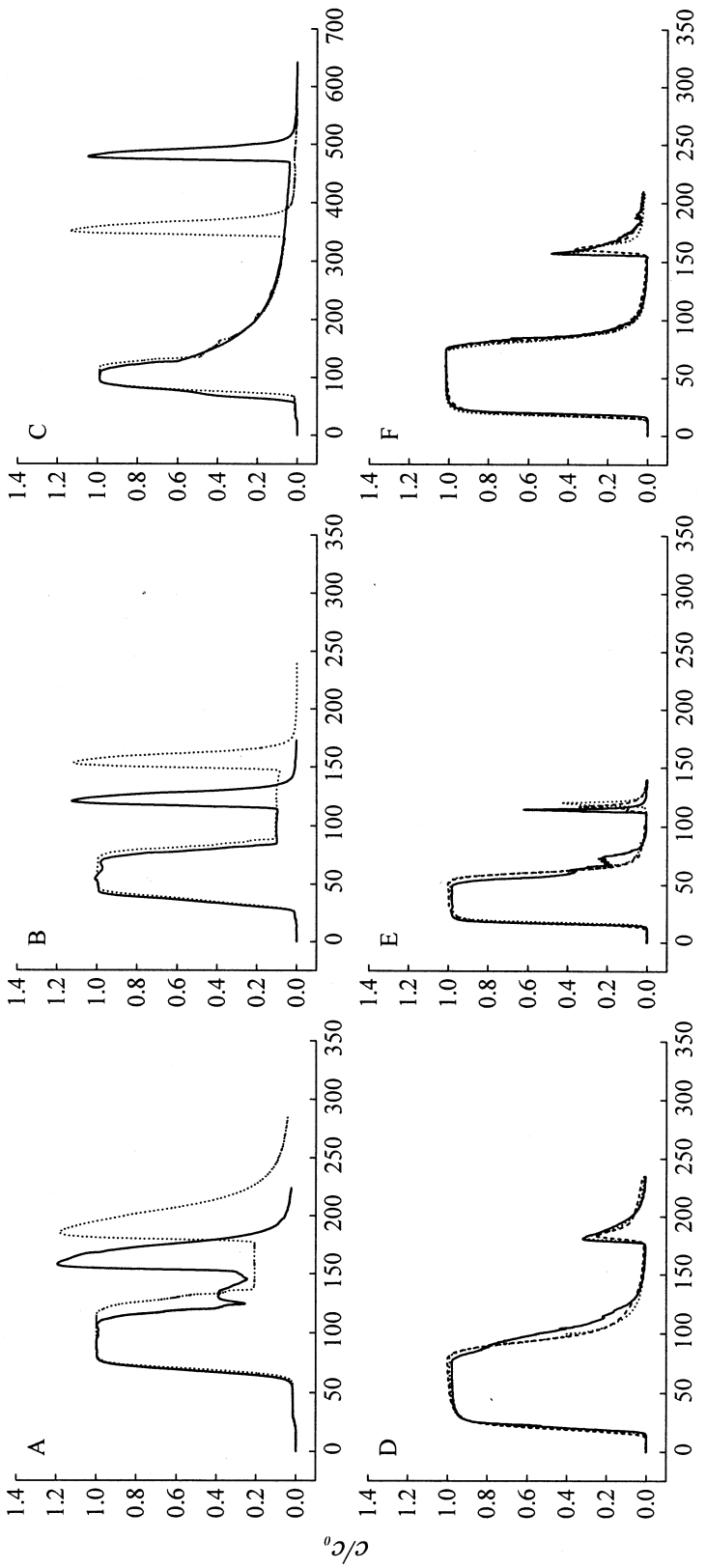

FIG. 3 Effect of flow rate on the breakthrough curves for single-protein experiments. Solid line = 0.5 mL/min; dotted line = 1 mL/min; dashed line = 5 mL/min. The settings for A to F are described in Table 2.

MARCEL DEKKER, INC.
270 Madison Avenue, New York, New York 10016

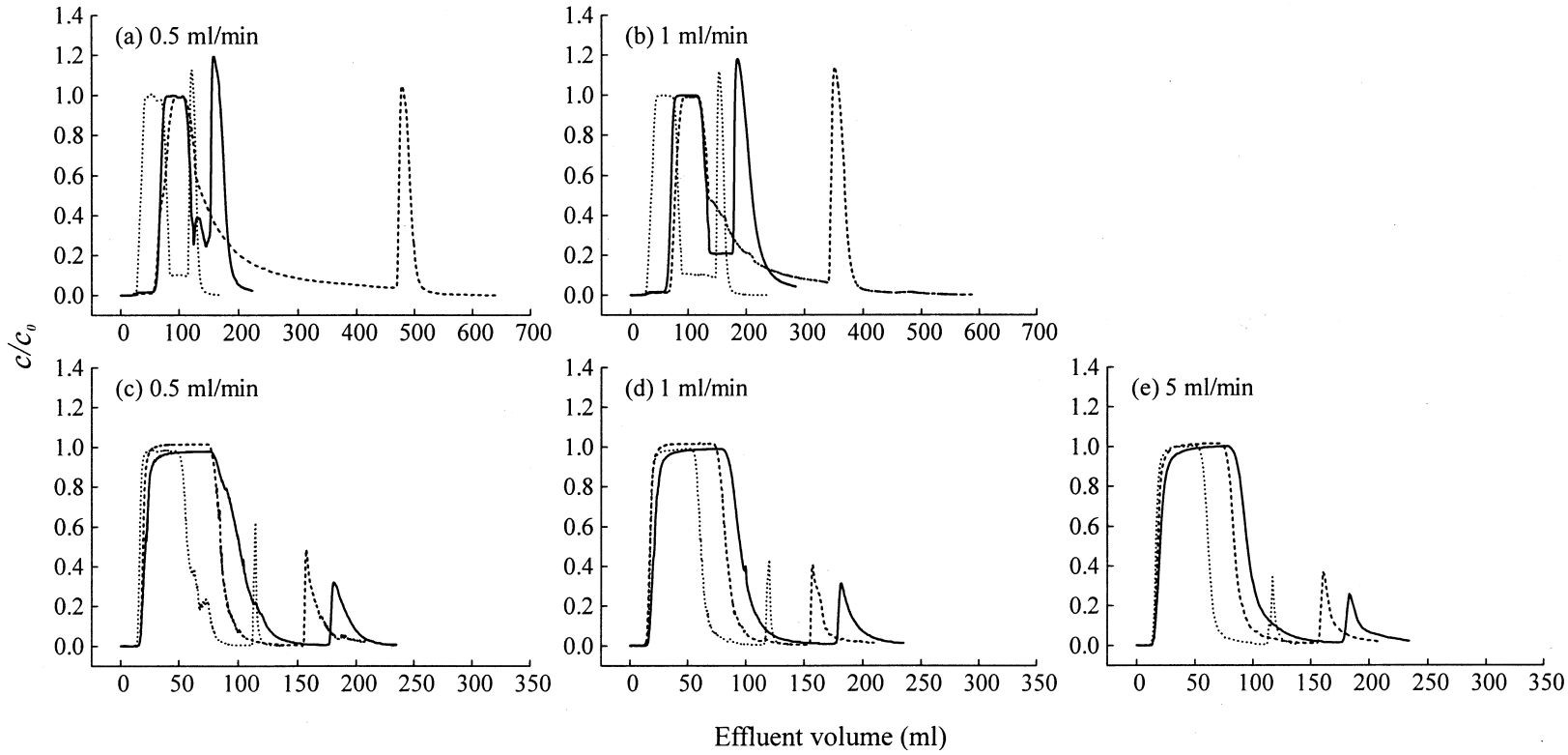

FIG. 4 Effect of different module designs on the breakthrough curves for single-protein experiments. For (a) and (b), solid line = setting A (wide and short column); dotted line = setting B (narrow and short column); dashed line = setting C (narrow and long column). For (c) to (e), solid line = setting D (wide and thin membrane stack); dotted line = setting E (narrow and thin membrane stack); dashed line = setting F (narrow and thick membrane stack). The settings for A to F are described in Table 2.

the BSA existed as a dimer and the rest as a monomer. It is worth recalling that both lysozyme and BSA could be bound onto the gel beads in the batch adsorption experiments, but only lysozyme was bound onto the membrane disks. Therefore, it can be expected that competitive adsorption of two proteins will occur for gel bead column experiments whereas a simple separation of lysozyme from BSA will occur in membrane performance. As observed from the experimental results, the above predictions for two-protein performance with different solid supports are valid. A detailed analysis will be presented in the following paragraphs.

For gel bead column performance, the adsorption behaviors presented in Fig. 5 resemble the model prediction of competitive adsorption combining local equilibrium theory and the extra-module effect in the literature (3). The breakthrough curve, governed basically by local equilibrium theory, contains square-wave plateaus where the solutes emerge in the effluent in the order of increasing affinity strength. At the beginning of loading, all the affinity solutes are completely bound to the ligand and no solute will emerge in the effluent. As the binding sites are saturated, the stronger-affinity solutes start to displace the bound lowest-affinity solute out of the support surface. This displacement will result in an effluent concentration of lowest-affinity solute higher than its feed concentration, and it will form the first plateau in the breakthrough curve. When the binding sites are saturated again with the affinity solutes, except for the lowest-affinity one, it becomes the turn for the second lowest-affinity so-

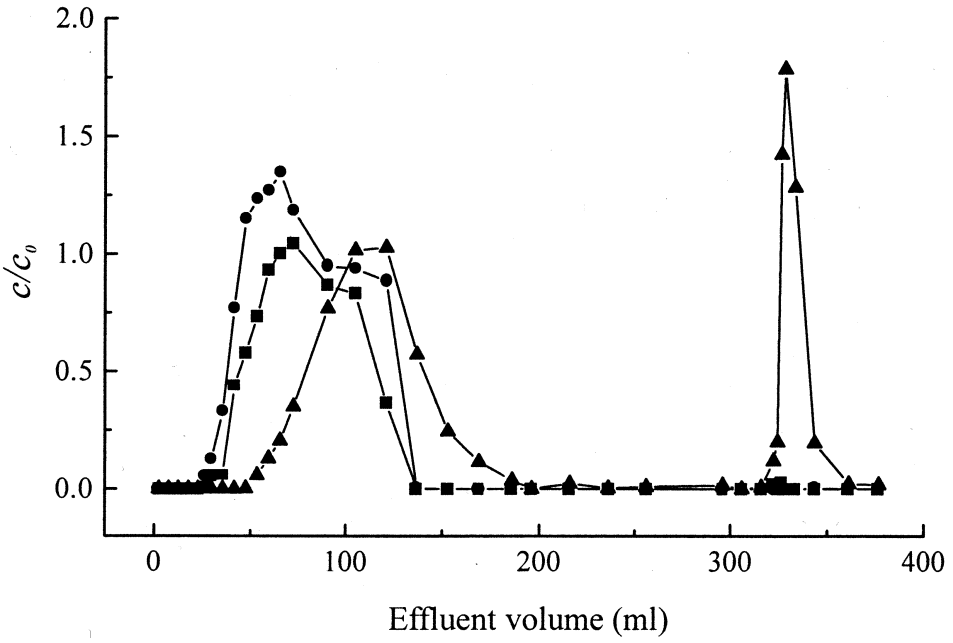

FIG. 5 Two-protein breakthrough curves using gel bead column at setting B and 1 mL/min. Solutes: (■) BSA dimer; (●) BSA monomer; (▲) lysozyme.

MARCEL DEKKER, INC.
270 Madison Avenue, New York, New York 10016

lute to be displaced, and the second plateau then results. The same procedure will be repeated again and again until the solid support is saturated mostly with the highest-affinity solute and final equilibrium is reached. Displacement will then stop and all the solutes will emerge in the effluent with their feed concentration. The extra-module effect broadens the edges of the square waves and decreases the effluent concentration during displacement.

In Fig. 5, BSA monomer first emerged with a peak effluent concentration around 1.35-fold of the feed concentration. BSA dimer came out second with a peak concentration 1.05 times that of the feed. Lysozyme emerged last, and the effluent concentration returned to a steady concentration at an effluent volume of 100 mL for these three solutes. The steady concentrations were 1.02, 0.94, and 0.85 of the feed for lysozyme, BSA monomer, and BSA dimer, respectively. As explained by local equilibrium theory, the final equilibrium concentrations should return to those of the feed. It may be due to experimental errors that the concentrations did not reach the feed concentrations for BSA solutes. Lysozyme and BSA dimer showed broader curves than BSA monomer in the washing curves.

Based on the order of emergence in the effluent as explained by local equilibrium theory, the affinity strength to the gel bead support should be: lysozyme $>$ BSA dimer $>$ BSA monomer. However, this result is opposite to that of batch adsorption experiments where BSA exhibited a higher affinity strength. Two possible reasons may explain this contradiction. One is that the result in the batch experiment was for BSA monomer and dimer together, which may be different from the behavior for each single BSA solute. In addition, the adsorption behavior of each protein in a competitive two-protein adsorption environment may be different from its behavior in a single-protein environment, as demonstrated in the literature (15). Therefore, it may be inaccurate to use the results from the single-protein experiments to predict the multiprotein behaviors. Another noticeable point is that lysozyme had a saturation capacity 10 times higher than BSA in the batch adsorption results. Not only affinity strength but also adsorption saturation capacity can affect the overall adsorption behavior. In this case the effect of saturation capacity may be more dominant in the competitive adsorption performance than the effect of affinity strength. This can be verified in the elution result which shows that the elution peak collected is mostly from lysozyme. In other words, almost no BSA was adsorbed on the gel beads after the competition.

The two-protein performance using membrane disks as the solid support is illustrated in Fig. 6. Recalling that only lysozyme could bind in the batch adsorption experiment, a simple separation for only lysozyme adsorbed can be expected. The resulting breakthrough curves exactly demonstrate this trend. BSA monomer and dimer emerged first, and the effluent concentration rose to a value about 90% of their feed and then remained steady. BSA dimer had a broader breakthrough curve than monomer. These two BSA solutes did not

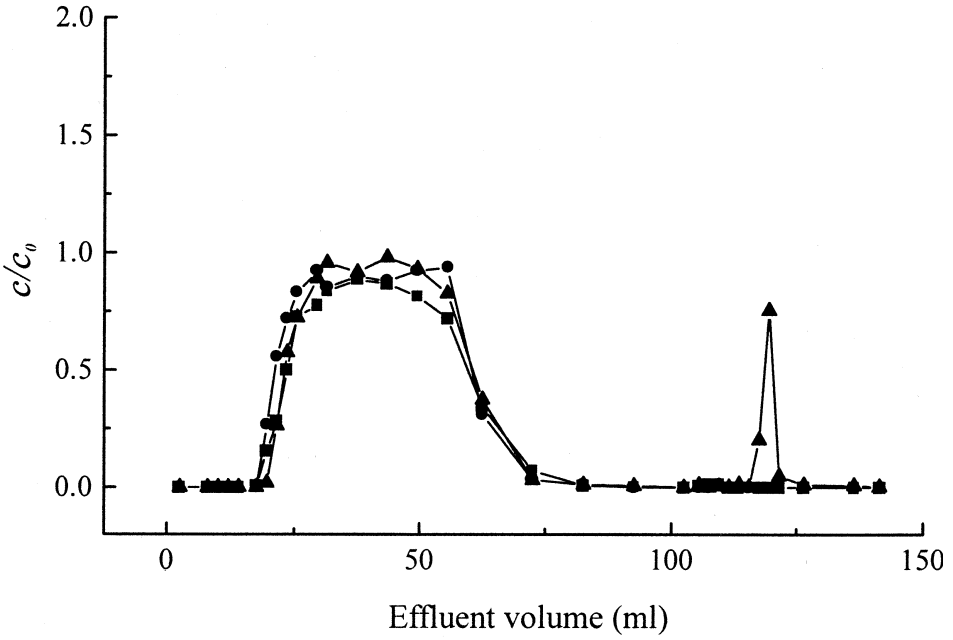

FIG. 6 Two-protein breakthrough curves using membrane disks at setting E and 1 mL/min. Solutes: (■) BSA dimer; (●) BSA monomer; (▲) lysozyme.

adsorb onto membranes, so their displacement by lysozyme would not happen. Consequently, BSA effluent concentrations did not exceed the corresponding feed concentrations. Lysozyme emerged last, but its curve was quite close to that for BSA dimer. The effluent concentration of lysozyme rose to 98% of the feed concentration. The final elution peak contained only lysozyme.

Varied performance was observed by comparing the breakthrough curves of the same two proteins using different solid supports. However, either in the case of competitive adsorption (both proteins bound, but with different affinity strengths and different saturation capacities) or in the case of simple separation (only one protein bound), almost pure lysozyme was collected in the elution stage. From this point of view, a good separation could be performed in both the gel bead column and membrane disk processes. However, from another standpoint, the BSA separation performance was different in various processes. Pure BSA could not be separated using membranes due to the close emergence of different proteins, but it could be fractionally collected in the effluent during the loading stage if a gel bead column was used. This advantage suggests that column design may be a better choice for practical use. To overcome the close-emergence problem for membranes, a greatly increasing membrane thickness is necessary. The thicker the membranes, the larger the amount of lysozyme required to load for adsorption. This will prolong the

overall adsorption time of lysozyme and lead to a larger offset in the emergence period between lysozyme and BSA.

To investigate the process efficiency, the cycle time, the loaded protein amount, and the adsorbed protein amount were also examined for both the column and membrane processes. From Figs. 5 and 6, around 275 mL of effluent volume (about 54 bed volumes) was needed for a separation cycle of the column process with 5.1 cm^3 bed volume, and 75 mL of effluent volume (about 174 bed volumes) for a cycle of the membrane process with 0.43 cm^3 bed volume. These values were obtained from the total volume shown in the figures by subtracting the unnecessary waiting volume. In a cycle, 100 mL of protein solution was loaded for the column process and 15 mL as needed for loading in the membrane process. Similarly, these values were calculated by subtracting the unnecessary waiting volume from the actual loading volume. Then, the loaded lysozyme amounts were 200 mg for the column process and 30 mg for the membrane process based on the calculation of the loading volume multiplied by a lysozyme feed concentration of 2 mg/mL. The corresponding adsorbed protein amounts were about 48 mg for the column process and 4.5 mg for the membrane process, obtained from the amount of protein collected in the elution stage in Figs. 5 and 6. Accordingly, the percentages recovered were 24% for the column process and 15% for the membrane process. Column performance was superior to membrane disks in this category for its shorter cycle time and higher recovery. On the other hand, around 3.7 cycles of the membrane process can be conducted in one column cycle based on the same effluent volume. This leads to around 16.5 mg of lysozyme totally recovered for the membrane process in the cycle time of one column. Compared to the 48 mg protein recovered in the column process, the total amount of protein recovered in the membrane process is still lower. These limitations partially come from the membrane thickness restriction of the membrane holder used in this work. A better membrane disk holder design to accommodate a thicker membrane stack is required for more efficient protein separation performance.

CONCLUSIONS

The breakthrough curve performance of lysozyme and BSA to immobilized Cibacron Blue 3GA using gel beads and membrane disks as solid supports was investigated. The effects of flow rate and different designs were also studied. The effect of flow rate was insignificant for both the column and membrane processes in nonadsorption experiments. However, the nonadsorption breakthrough curves of gel bead columns were broader than those of membrane disks, basically because of BLMT and intraparticle diffusion effects. Moreover, the results from various designs showed that the dominant factor affect-

MARCEL DEKKER, INC.
270 Madison Avenue, New York, New York 10016

ing nonadsorption breakthrough curves was column length for column separation and membrane diameter for the membrane process.

In single-protein experiments the effect of flow rate was also negligible for the column process but it affected the elution peak height for the membrane process. The peak height decreased with increasing flow rate. As to the effect of different designs, the trends were similar to those of the nonadsorption experiments: a long column and a wide membrane stack showed a broader performance.

In two-protein experiments the protein system was essentially a ternary-solute system because BSA existed as both the dimer and monomer. Comparison of breakthrough curves using different solid supports gave a varied performance. Competitive adsorption occurred for a gel bead column whereas a simple separation of lysozyme from BSA was observed for membrane performance. The breakthrough curve performance for a gel bead column resembled the prediction of combining local equilibrium theory and the extra-module effect, and the affinity strength to the support was found in the following order: lysozyme $>$ BSA dimer $>$ BSA monomer, based on their emergence in the effluent. As for membrane performance, the two BSA solutes did not adsorb onto membranes, so the displacement phenomena did not occur.

Using calculated values of the cycle time, loaded protein amount, and adsorbed protein amount to investigate process efficiency, column performance was superior to membrane disks because of its shorter cycle time and higher recovery percentage. The limitations of membrane performance came partially from the design of the membrane holder.

The investigation of breakthrough curve performance and the subsequent suggestions in this work may provide useful guidelines for a better design of membrane disk separations and a better choice for more suitable solid supports.

SYMBOLS

c	solute concentration in solution (μM)
c_l	saturation capacity based on the solid volume (μM)
c_s	adsorbed solute concentration based on the solid volume (μM)
d_p	membrane pore size (cm)
D	diffusion coefficient ($cm^2 \cdot min^{-1}$)
D_p	particle diameter (cm)
k_c	BLMT coefficient ($cm \cdot min^{-1}$)
K_d	dissociation equilibrium constant (μM)
L	bed length (cm)
v	interstitial velocity ($cm \cdot min^{-1}$)

MARCEL DEKKER, INC.
270 Madison Avenue, New York, New York 10016

REFERENCES

1. S. Brandt, R. A. Goffe, S. B. Kessler, J. L. O'Connor, and S. E. Zale, "Membrane-Based Affinity Technology for Commercial Scale Purifications," *Bio/Technology*, *6*, 779 (1988).
2. K.-G. Briefs and M.-R. Kula, "Fast Protein Chromatography on Analytical and Preparative Scale Using Modified Microporous Membranes," *Chem. Eng. Sci.*, *47*, 141 (1992).
3. S.-Y. Suen and M. R. Etzel, "Sorption Kinetics and Breakthrough Curves for Pepsin and Chymosin Using Pepstatin A Affinity Membranes," *J. Chromatogr. A*, *686*, 179 (1994).
4. J. Thommes and M.-R. Kula, "Membrane Chromatography—An Integrative Concept in the Downstream Processing of Proteins," *Biotechnol. Prog.*, *11*, 357 (1995).
5. D. K. Roper and E. N. Lightfoot, "Separation of Biomolecules Using Adsorptive Membranes," *J. Chromatogr. A*, *702*, 3 (1995).
6. C. Charcosset, "Purification of Proteins by Membrane Chromatography," *J. Chem. Technol. Biotechnol.*, *71*, 95 (1998).
7. W. F. Weinbrenner and M. R. Etzel, "Competitive Adsorption of α-Lactalbumin and Bovine Serum Albumin to a Sulfopropyl Ion-Exchange Membrane," *J. Chromatogr. A*, *662*, 414 (1994).
8. W. Guo, Z. Shang, Y. Yu, and L. Zhou, "Membrane Affinity Chromatography of Alkaline Phosphatase," *Ibid.*, *685*, 344 (1994).
9. H.-C. Liu and J. R. Fried, "Breakthrough of Lysozyme through an Affinity Membrane of Cellulose-Cibacron Blue," *AIChE J.*, *40*, 40 (1994).
10. J. E. Kochan, Y.-J. Wu, and M. R. Etzel, "Purification of Bovine Immunoglobulin G via Protein G Affinity Membranes," *Ind. Eng. Chem. Res.*, *35*, 1150 (1996).
11. E. Klein, D. Yeager, R. Seshadri, and U. Baurmeister, "Affinity Adsorption Devices Prepared from Microporous Poly(amide) Hollow Fibers and Sheet Membranes," *J. Membr. Sci.*, *129*, 31 (1997).
12. A. Denizli, D. Tanyolac, B. Salih, E. Aydinlar, A. Ozdural, and E. Piskin, "Adsorption of Heavy-Metal Ions on Cibacron Blue F3GA-Immobilized Microporous Polyvinylbutyral-Based Affinity Membranes," *Ibid.*, *137*, 1 (1997).
13. M. Weissenborn, B. Hutter, M. Singh, T. C. Beeskow, and F. B. Anspach, "A Study of Combined Filtration and Adsorption on Nylon-Based Dye-Affinity Membranes: Separation of Recombinant L-Alanine Dehydrogenase from Crude Fermentation Broth," *Biotechnol. Appl. Biochem.*, *25*, 159 (1997).
14. K. H. Gebauer, J. Thommes, and M.-R. Kula, "Breakthrough Performance of High-Capacity Membrane Adsorbers in Protein Chromatography," *Chem. Eng. Sci.*, *52*, 405 (1997).
15. S.-Y. Suen and Y.-S. Chang, "Adsorption and Desorption of Lysozyme and Albumin to Cibacron Blue 3GA Using Gel Beads and Membrane Discs," *J. Chin. Inst. Chem. Eng.*, *29*, 307 (1998).
16. P. M. Boyer and J. T. Hsu, "Effects of Ligand Concentration on Protein Adsorption in Dye-Ligand Adsorbents," *Chem. Eng. Sci.*, *47*, 241 (1992).
17. S.-Y. Suen and M. R. Etzel, "A Mathematical Analysis of Affinity Membrane Bioseparations," *Ibid.*, *47*, 1355 (1992).

Received by editor April 7, 1999
Revision received July 1999

MARCEL DEKKER, INC.
270 Madison Avenue, New York, New York 10016

Request Permission or Order Reprints Instantly!